Mechanics Research Communications 72 (2016) 74–80

Contents lists available at ScienceDirect

Mechanics Research Communications

journal homepage: www.elsevier.com/locate/mechrescom

Rotation control of a parametrically excited pendulum by adjusting its length

Florencia Reguera [a], Franco E. Dotti [b,*], Sebastián P. Machado [b]

[a] Grupo de Investigación en Multifísica Aplicada, Universidad Tecnológica Nacional, Facultad Regional Bahía Blanca, Consejo Nacional de Investigaciones Científicas y Técnicas, Departamento de Ingeniería, Universidad Nacional del Sur, Argentina
[b] Grupo de Investigación en Multifísica Aplicada, Universidad Tecnológica Nacional, Facultad Regional Bahía Blanca, Consejo Nacional de Investigaciones Científicas y Técnicas, Argentina

ARTICLE INFO

Article history:
Received 9 October 2015
Received in revised form 5 January 2016
Accepted 26 January 2016
Available online 4 February 2016

Keywords:
Energy harvesting
Parametric pendulum
Length adjustment
Wave energy

ABSTRACT

We present a new control strategy for the vertically excited parametric pendulum, with a view on energy harvesting from rotating motion. Two possible energy sources are considered: a vibrating machine, represented by a sinusoidal excitation; and the sea waves, simulated by a stochastic process. In both cases, rotations can be achieved and maintained only for some forcing conditions. Thus, as stable rotations are required, the pendulum must be controlled. We propose to perform this control by means of a telescopic adjustment of the pendulum length during the motion. The idea is to give the pendulum an aid to reach and maintain rotations, accelerating the motion by modifying conveniently the position of the mass. To a better understanding of this concept, one may think of a child on a swing, who extends or retracts his legs in order to accelerate the motion. Numerical simulations show that, with a control action of this kind, stable rotations can be reached regardless of the forcing conditions and for every set of initial conditions. These are very promising results in terms of energy harvesting, since an optimized application of this control technique can lead to the design of autonomous pendulum harvester devices.

© 2016 Elsevier Ltd. All rights reserved.

1. Introduction

The increasing global awareness about the environmental damage has prompted in recent years the search for clean energy sources. The vast energy availability in ambient vibrations allows the development of many systems, aimed at the recovery of energy from variety of sources. These sources include the motion of large bodies of water [1,2], the biomechanics of a walking person [3] and the vibrations in civil structures [4], industrial machines [5] or flying planes [6], among others [7–9].

The vertical parametric pendulum was firstly proposed as an energy harvester device by Prof. Marian Wiercigroch [2]. Since the beginning of the century, he and his co-workers, and also other scientists, explored the ability of such systems for energy extraction from the ocean waves [10–16]. The idea consists of a pendulum on a floating platform, which is in turn vertically excited by the waves at a given (averaged) frequency. If stable rotational motion is achieved, a generator attached to the pendulum axis may produce electrical energy [12]. Although the idea is very simple and intuitive, its implementation is not trivial since stable rotations may be difficult to obtain, even with a simple sinusoidal excitation [17]. This is due to a strong dependence on forcing parameters and initial conditions of position and velocity. Thus, to reach stable rotations, a control strategy is necessary [11].

One of the forcing conditions we consider in this work is a sinusoidal excitation, with constant forcing parameters of amplitude and frequency. This situation can represent the motion imposed to the pendulum by an industrial vibrating machine. In this case, stable pure rotations (i.e. no oscillating behavior of any kind, [18]) can be reached only for some combinations of the forcing parameters [17]. But even if these parameters can be conveniently chosen, rotations coexist with other responses such as oscillations and chaotic motion, depending on the initial conditions [19]. Moreover, it has been demonstrated [12] that, in practical terms, stable pure rotations are possible only in a subset of the theoretical region of the parameter space. Being the forcing parameters constant, part of the problem can be solved with an adequate design, by tuning the system within the region of the parameter space in which rotations are possible. With a good design, control of rotations is required only to correct responses due to unsuitable initial conditions.

The other excitation considered is the motion of the sea waves, which is simulated as a stochastic process [11]. In this situation,

* Corresponding author. Tel.: +54 291 455 5220; fax: +54 291 455 5311.
E-mail address: fdotti@frbb.utn.edu.ar (F.E. Dotti).

http://dx.doi.org/10.1016/j.mechrescom.2016.01.011
0093-6413/© 2016 Elsevier Ltd. All rights reserved.

there are multiple forcing parameters of amplitude and frequency (determined by a spectral density), and there is not a suitable design for tuning the system. The response of the pendulum is also stochastic, and active control is necessary not only to ensure rotational response irrespective of initial conditions, but also to deal with a continuously changing load.

We propose an active control by means of an actuator, which adjusts the pendulum length during the motion. This idea has been successfully applied for a simple damped pendulum [20]. The telescopic adjustment gives the pendulum an aid to reach and maintain rotations, accelerating the motion by modifying the position of the mass according to a convenient strategy. The control function proposed to govern the change of length uses as input the measurement of the angle and velocity of the pendulum. Since rotations produce arbitrary large angle values, a sine function is used in order to keep the rotation control as dependent on the angular position but not on the actual angle measurement. The dependence on angular velocity is modeled with a logistic function, which value depends on whether velocity adopts positive or negative values. The application of the control is limited by a predefined threshold velocity, and steepness factors are defined to get a realistic value for the actuator velocity.

The article is organized as follows. After this introduction (Section 1), the equation of motion of the vertical parametric pendulum with variable length is derived, considering sinusoidal and stochastic excitations (Section 2). Then, the control strategy employed to adjust the pendulum length is presented and explained (Section 3). Finally, the results of numerical simulations comparing controlled and uncontrolled pendulums are presented and discussed (Section 4).

2. The vertical parametric pendulum with variable length

2.1. Equation of motion

Consider the pendulum system given in Fig. 1, which axis of rotation is excited by an imposed motion $Y = Y(t)$. The total length of the pendulum, l, can be modified by adjusting the position of the telescopic rod, of length l_2. When this rod is retracted, the pendulum recovers its natural length l_1 ($l = l_1$). The equation of motion of this system can be set up by using Lagrange's equation for single degree-of-freedom non-conservative systems, which can be expressed as.

$$\frac{d}{dt}\left(\frac{dT}{d\dot{\theta}}\right) - \frac{dT}{d\theta} + \frac{dV}{d\theta} + \frac{dD}{d\dot{\theta}} = 0 \tag{1}$$

where θ is the angle measured from the downward hanging position (positive in counter-clockwise direction), while T, V and D represent kinetic, potential and dissipative energy of the system, respectively. These energy magnitudes are

$$\begin{aligned} T &= \frac{m}{2}\left[\left(l\dot{\theta}\cos\theta\right)^2 + \left(\dot{Y} + l\dot{\theta}\sin\theta\right)^2\right] \\ V &= mgl(1-\cos\theta) \\ D &= \frac{1}{2}c_\theta l^2\dot{\theta}^2 \end{aligned} \tag{2}$$

where m is the mass of the bob, c_θ is the viscous damping coefficient and g the acceleration of gravity.

Introducing Eq. (2) into Eq. (1) and performing the corresponding derivatives, the equation of motion of the system can be obtained as

$$ml^2\ddot{\theta} + m(l\ddot{Y} + lg + \dot{l}\dot{Y})\sin\theta + (c_\theta l^2 + 2m\dot{l}l)\dot{\theta} = 0 \tag{3}$$

where $\dot{l}$ represents physically the linear velocity of the telescopic actuator. Eq. (3) allows studying the dynamics of the pendulum for an arbitrary time-dependant imposed motion Y.

2.2. Imposed motion as a sinusoidal wave

If the imposed motion is a wave of the form $Y(t) = -A\cos(\Omega t)$, Eq. (3) takes the form (after dividing by ml^2)

$$\ddot{\theta} + \left(\frac{c_\theta}{m} + 2\frac{\dot{l}}{l}\right)\dot{\theta} + \frac{1}{l}\left[A\Omega^2\cos(\Omega t) + g + \frac{\dot{l}}{l}A\Omega\sin(\Omega t)\right]\sin\theta = 0 \tag{4}$$

For l constant, Eq. (4) recovers the classical equation of motion of the vertical parametric pendulum [17,21].

2.3. Imposed motion as a simulated sea wave

A sea wave can be represented by a composition of sinusoidal waves with frequencies determined by a spectral density. To simulate the time history of a wave, we use the approach presented in reference [11], based on the Shinozuka–Jan method for random processes [22] and the Pierson–Moskowitz spectral representation of the sea waves [23]. This power spectral density is given by

$$S(\Omega) = \frac{8.1g^2}{10^3\Omega^5}\exp\left(-0.032\frac{g^2}{\Omega^4 H_s^2}\right) \tag{5}$$

where H_s is the significant wave height, corresponding to 1/3 of the highest wave measured. With the statistical information of Eq. (5), the stochastic time-dependant excitation of the sea wave is expressed as

$$Y(t) = \sqrt{2}\sum_{i=1}^{N}\sqrt{(\Omega_i - \Omega_{i-1})S(\Omega_i)}\cos(\Omega_i t + \phi_i) \tag{6}$$

where ϕ_i are random phase angles and N is the number of sampled frequencies. The frequency range, $[\Omega_0, \Omega_N]$ must be set in a way that most of the spectrum S to be contained at that range. The frequency intervals, $\Omega_i - \Omega_{i-1}$, are determined by solving the following equation

$$\int_{i-1}^{i} S(\Omega)d\Omega = \int_{i}^{i+1} S(\Omega)d\Omega \tag{7}$$

The fulfillment of Eq. (7) ensures that the area under the curve of $S(\Omega)$ is the same for all frequency intervals, with the consequent good covering of the highest spectral density zone. The wave model of Eq. (6) was tested against real data, producing a good agreement [11]. Considering Eq. (6) as the imposed motion required in Eq. (3), we can study the behavior of the pendulum with adjustable length under the excitation of the sea waves.

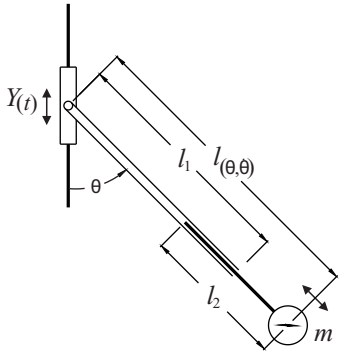

Fig. 1. Scheme of the vertical parametric pendulum with variable length.

3. Control strategy

3.1. Control function

The main goal of the approach is to give the parametric pendulum an aid to reach and maintain pure rotations, by means of a telescopic adjustment of the pendulum length during the motion. This adjustment must be appropriate in order to accelerate the angular motion of the pendulum when necessary. At first we attempted to employ the control technique presented in [20], which seems to work well for the simple damped pendulum. This technique is represented by the equation

$$l(\theta, \dot{\theta}) = l_1 + \tfrac{1}{2} l_2 (1 - \theta\dot{\theta}) \tag{8}$$

where $\theta\dot{\theta}$ is responsible for the acceleration. In [20] the authors consider the following situation: the pendulum is accelerated only by varying its length, until the first revolution is reached. When $|\theta| > \pi$, the sign of the nonlinear term $\theta\dot{\theta}$ is inverted in order to decelerate the pendulum, until it stops at the rest position. For this application, the control action of Eq. (8) produces good results. But with energy extraction purposes, pure rotations not only have to be reached but also maintained, resulting in a strictly growing angle θ. Moreover, $\dot{\theta}$ also can adopt high absolute values (indeed, in order to optimize energy extraction, a small damping is desired which may lead to very high values of $\dot{\theta}$ [10]). In these terms, Eq. (8) generates unphysical values of l and $\dot{l}$. Another significant fact is that the energy necessary for the operation of the control must be extracted from the rotational motion of the pendulum. Thus, the control must be set to act for the shortest time possible. Eq. (8) does not allow applying such restriction. Given these drawbacks, we modify Eq. (8) as follows

$$l(\theta, \dot{\theta}) = l_1 + l_2 \cdot \psi(\theta, \dot{\theta}) \tag{9}$$

where the control function is

$$\psi(\theta, \dot{\theta}) = \tfrac{1}{2}[1 - p_\theta(\theta) \cdot p_{\dot{\theta}}(\dot{\theta})] \cdot \varphi(\dot{\theta}) \tag{10}$$

and

$$p_\theta(\theta) = \sin\theta \tag{11}$$

$$p_{\dot{\theta}}(\dot{\theta}) = 2[1 + \exp(-k\dot{\theta})]^{-1} - 1 \tag{12}$$

$$\varphi(\dot{\theta}) = \{1 + \exp[-k_L(\dot{\theta} - \dot{\theta}_L)]\}^{-1} - \{1 + \exp[-k_L(\dot{\theta} + \dot{\theta}_L)]\}^{-1} \tag{13}$$

The functions p_θ and $p_{\dot{\theta}}$ represent the dependence of l on θ and $\dot{\theta}$, respectively. Being a sine, p_θ ensures that the change of length l is independent of how large θ could be. Meanwhile, $p_{\dot{\theta}}$ is a logistic function and its value depends on whether $\dot{\theta}$ is positive or negative. The coefficient k of Eq. (12) is a steepness factor and must be set in order to get a realistic value of the actuator velocity $\dot{l}$ when $\dot{\theta}$ passes through zero.

The energy required for the control must be obtained from the power generation since the pendulum system is supposed to be autonomous. Thus, the operating time of the control must be the shortest possible, in order to make the technology viable (in fact, this is a latent optimization problem which is not addressed in this article). The function φ of Eq. (13) regulates the application of the control action, in the following form: being $\dot{\theta}_L$ a predefined threshold velocity, while $|\dot{\theta}| > \dot{\theta}_L$ the pendulum is assumed to be rotating, and therefore its length must not be adjusted, then $\varphi = 0$ and l keeps constant ($l = l_1$); otherwise ($|\dot{\theta}| < \dot{\theta}_L$), φ can adopt values different than zero and thus l is controlled according to Eq. (9). In order to get a realistic model, the transition at $|\dot{\theta}| = \dot{\theta}_L$ must be smooth. This transition is governed by adequately setting the coefficient k_L.

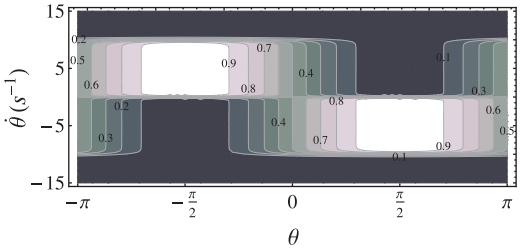

Fig. 2. Example of the control function ψ. $\dot{\theta}_L = 10\,s^{-1}$, $k = 10$ and $k_L = 5$.

A contour plot of an example control function ψ is presented in Fig. 2. It can be seen that if $|\dot{\theta}| \gtrsim \dot{\theta}_L$ or $\text{sign}(\theta) = \text{sign}(\dot{\theta})$ (both possible rotating scenarios), then φ tends to be zero. On the other hand, if $|\dot{\theta}| \lesssim \dot{\theta}_L$ and $\text{sign}(\theta) \neq \text{sign}(\dot{\theta})$, there is an oscillating scenario and thus φ tends to be one in order to increase l and accelerate the motion (see Eq. (9)).

3.2. Setting the threshold angular velocity

The threshold angular velocity $\dot{\theta}_L$ is a key parameter in terms of energy savings in the control action. This velocity must be defined a priori. It has been stated that if $|\dot{\theta}| \gtrsim \dot{\theta}_L$ the pendulum is assumed to be rotating, and therefore its length must not be adjusted. Since setting $\dot{\theta}_L$ is not trivial, we conduct a numerical experiment on the undriven damped pendulum in order to obtain a simple formula to make an estimation of this reference value. The equation of the undriven pendulum is given by

$$\ddot{\theta} + \frac{c_\theta}{m}\dot{\theta} + \frac{g}{l_1}\sin\theta = 0 \tag{14}$$

which can be recovered from Eq. (4) by setting $l = l_1$, $\dot{l} = 0$ and $A = 0$. In order to gain in generality, Eq. (14) can be non-dimensionalized as

$$\theta'' + \beta\theta' + \sin\theta = 0 \tag{15}$$

where $\beta = c_\theta/(m\omega_0)$ is the non-dimensional damping coefficient and $\omega_0 = \sqrt{q/l_i}$ is the natural frequency of the retracted system ($l = l_1$). $(\bullet)'$ denotes differentiation with respect to the non-dimensional time $\tau = \omega_0 t$. Now, for different values of the initial (non-dimensional) velocity θ'_0, we solve Eq. (15) searching for the minimal θ'_0 which allows reaching $|\theta| > \pi$, starting from the rest position ($\theta_0 = 0$).

The results of this numerical experiment, performed for different values of β, are presented in Fig. 3. It is clear that the relation between the minimal $|\theta'_0|$ (necessary to reach at least one rotation from the rest position) and β is linear. This relation can be approximated as

$$|\theta'_{0,\min}| = 2(1.1\beta + 1) \tag{16}$$

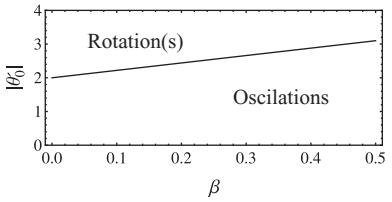

Fig. 3. Threshold of θ'_0 for rotations of the damped undriven pendulum as a function of the non-dimensional damping coefficient β. The initial angular position is the rest position ($\theta_0 = 0$). Absolute value of velocity is plotted given the symmetry of the system: clockwise or counter-clockwise rotations are equally achieved.

For given values of β and the initial conditions $\theta_0 = 0$ and θ_0', if $|\theta_0'| > |\theta_{0.\,\min}'|$ then the undriven damped pendulum reaches $|\theta| > \pi$. From Eq. (16) and since $|\dot{\theta}| > \omega_0|\theta'|$, we can write

$$|\dot{\theta}_{0,\min}| = 2(1.1c_\theta m^{-1} + \omega_0) \tag{17}$$

and propose the following expression for the threshold angular velocity.

$$\dot{\theta}_L = \alpha_L|\dot{\theta}_{0,\min}| \tag{18}$$

where α_L is a weight parameter.

Eq. (18) gives a reference value to estimate the threshold of rotations of the parametric pendulum. Since it is derived from solving for a simpler physical system, it does not provide absolute certainty. We could state that if $|\dot{\theta}| > |\dot{\theta}_{0,\min}|$ rotations *may be lost* and therefore active control should act. But numerical experiments show that stable rotations can be reached for $0.5 < \alpha_L < 1$, so α_L has to be set based on the experience (lower α_L are desired to save energy in the control operation). For a sinusoidal excitation, a more accurate estimation for $\dot{\theta}_L$ could be done by performing a robustness analysis of the attractors, for example using the IF criterion [24]. But this way carries a high computational cost (it requires knowing the complete basin of attraction) and only can be justified for fixed forcing parameters A and Ω.

4. Numerical results and discussion

4.1. Overview

We present numerical comparisons between the behavior of the parametric pendulum with adjustable length and constant length. Both forcing scenarios presented in Section 2 are considered: a cosine wave and a simulated sea wave. The following dimensions are considered for all the examples: $l_1 = 0.27$ m, $l_2 = 0.05$ m and $m = 0.7$ kg, corresponding to a natural frequency of $\omega_0 = 6.028\ \mathrm{s}^{-1}$ for the retracted system (constant length, $l = l_1$). These dimensions are similar to those of the experimental device of reference [11]. Simulations are run up to a time of 2500 s to ensure stationary response.

4.2. Sinusoidal excitation

Consider the parametric pendulum with constant length, subjected to a sinusoidal excitation with forcing parameters A and Ω. If Eq. (4) is solved for l constant, one finds that rotations are possible only for some combinations of the forcing parameters. These combinations constitute a rotation zone in the parameter space A–Ω, whose boundaries were studied by Clifford and Bishop [17]. Since the boundaries also depend on the pendulum dimensions, an adequate design of the pendulum device allows setting the system into the rotation zone. But even with a design that makes rotations feasible, they coexist with other responses due to the strong dependence of the system on initial conditions.

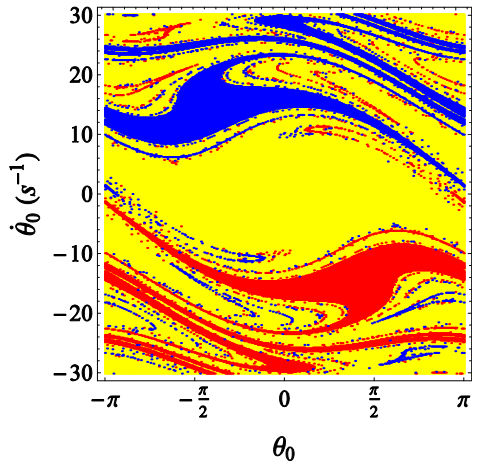

Fig. 4. Basin of attraction of the parametric pendulum with constant length ($l = l_1$). Imposed motion: $Y(t) = -A\cos(\Omega t)$, $A = 47.25$ mm, $\Omega = 12.05\ \mathrm{s}^{-1}$. (▬): anticlockwise rotations, (▬): clockwise rotations, (▬): oscillations. (The fractalization of the basin of oscillations is due to the occurrence of the homoclinic tangency, a typical phenomenon of systems involving escape from the potential well [25]).

This can be exemplified by the basin of attraction of Fig. 4, from where it can be noted that only a limited set of initial conditions $(\theta_0, \dot{\theta}_0)$ produce stable rotations. Thus, for a sinusoidal load, control of rotations is required only to correct responses due to unsuitable initial conditions.

Fig. 5 show a comparison between an uncontrolled pendulum (constant length, $l = l_1$) and a controlled pendulum by means of the length adjustment proposed in Eq. (9). We carefully choose the initial conditions from the basin of attraction of Fig. 4, ensuring that oscillatory motion is produced if the pendulum is not controlled. The damping is set as $c_\theta = 0.422$ kg/s, corresponding to $\beta = 0.1$, which is a usual value in experimental and theoretical works [17,26]. From the comparative plot of $\dot{\theta}$ (Fig. 5) it can be seen that the control action produces an increase of velocity during the oscillation, due to the adjustment of l. This happens until the first rotation is achieved, shortly after $t = 5$ s. Once rotations are reached the control action diminishes (l tends to l_1), and reactivates when rotations seem to lose ($|\dot{\theta}| \lesssim \dot{\theta}_L$, at $t \cong 8$ s and $t \cong 10.2$ s). When rotating motion

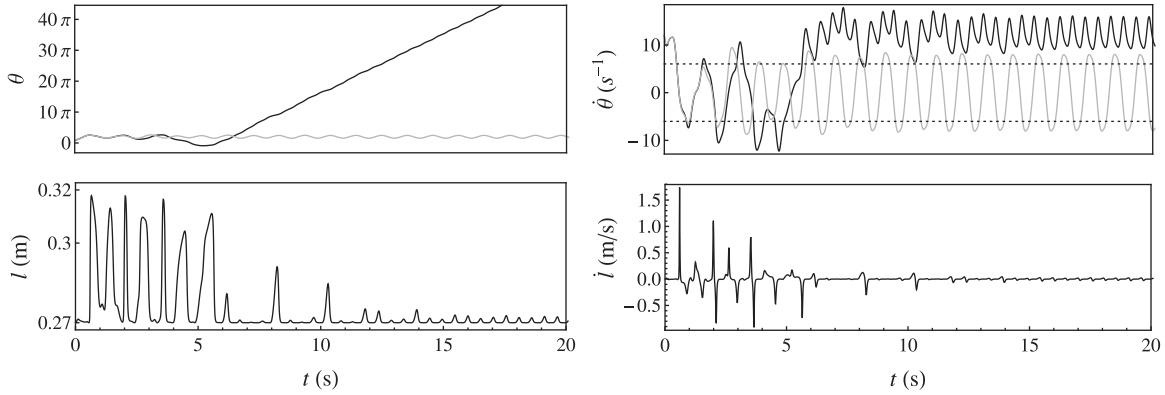

Fig. 5. Comparison between controlled (—) and uncontrolled (▬) responses of the parametric pendulum. Imposed motion: $Y(t) = -A\cos(\Omega t)$, $A = 47.25$ mm, $\Omega = 12.05\ \mathrm{s}^{-1}$. Initial conditions: $\theta_0 = 3\pi/4$, $\dot{\theta}_0 = 12\ \mathrm{s}^{-1}$. Steepness factors: $k = 2.5$, $k_L = 0.82$. Threshold factor: $\alpha_L = 0.45$, (. . .): $\dot{\theta}_L = 6.02\ \mathrm{s}^{-1}$. Counterclockwise rotations are successfully obtained due to the control action. For the uncontrolled pendulum, the response is oscillatory.

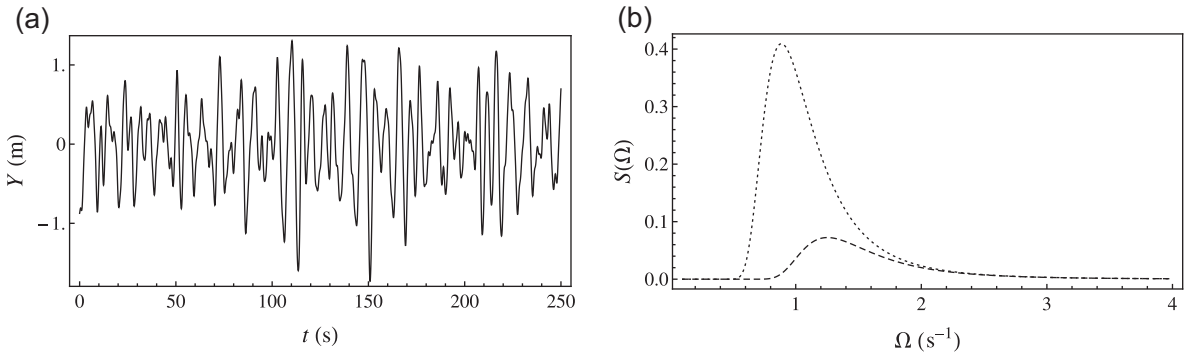

Fig. 6. (a) Simulation of the stochastic vertical motion applied to the pendulum system by the sea waves ($H_s = 2.0$ m) and (b) simulated power spectral density of the sea waves, (- -): $H_s = 1.0$ m, (. . .): $H_s = 2.0$ m.

stabilizes ($t > 15$ s), the control action disappears in practical terms ($l \cong l_1$).

It can also be observed from Fig. 5 that $\dot{l}$ does not exceed 2 m/s (the magnitude of $\dot{l}$ is governed by k and k_L). This makes a real application (for example, a vibrating industrial machine) viable, since a very fast actuator is considered to work at 3 m/s [20]. With the application of the control strategy, it is found that rotational motion never loses after 2500 s of simulation, irrespective of the initial conditions. This means that there is no need to know the basin of attraction of Fig. 4, which requires a lot of calculations or experiments, to reach stable rotations. Besides the simulation of Fig. 5, many more were conducted with successful results for several combinations of initial conditions and loading states, and even with a chaotic uncontrolled response. In order to save space, those are not presented here.

The control action of Eq. (9) also allows obtaining stable rotations if the pendulum system is outside the rotation zone suggested by Clifford and Bishop [17]. But in this case a very strong control action is necessary, which could make the technique unfeasible from an energy consumption point of view.

4.3. Sea wave excitation

In this section, we study the behavior of the parametric pendulum with variable length under the excitation of the sea waves. The analysis is performed by considering Eq. (6) as the imposed motion $Y(t)$ required by Eq. (3). Of course, this forcing scenario is much more complex than the previously studied. Being $Y(t)$ a sum of out-of-phase cosines, there are multiple forcing parameters of amplitude and frequency and also phase angles, which must be randomly chosen. There is not a *rotation zone* as in the case of sinusoidal load and thus active control is necessary not only to modify unsuitable initial conditions, but also to ensure rotational response under a load of stochastic nature.

Fig. 6(a) shows one of the simulations of the sea waves ($H_s = 2$ m). To obtain such response, a total of $N = 50$ frequency components are considered in Eq. (6), which is equivalent to consider the continuous spectrum [11]. The sampling frequency range is set to (Ω_0, Ω_N) = (0, 4 s^{-1}). Fig. 6(b) allows verifying that most of the spectrum S is contained at that range. Two realistic values of the significant wave height are considered: $H_s = 1$ m and $H_s = 2$ m. The damping is set as $c_\theta = 0.01219$ kg/s, as in ref. [14].

Fig. 7 shows a comparison between an uncontrolled pendulum (constant length, $l = l_1$) and a controlled pendulum with adjustable length, both subjected to the forcing of Fig. 6(a), corresponding to $H_s = 2$ m. For the uncontrolled pendulum, the response is a fading oscillatory motion, reaching (in practical terms) the rest position $\theta = 0$ at $t \cong 150$ s. But with the length adjustment, rotations are reached and maintained.

If a comparison is made among plots of l of Figs. 5 and 7, it can be seen that the control must be much more operative for maintaining rotations when a stochastic sea motion is considered, instead of a sinusoidal excitation. This is logical (and unavoidable) since under stochastic loading the threshold condition $|\dot{\theta}| \dot{<} \dot{\theta}_L$ is much more frequent.

The example of Fig. 8 presents a scenario of high initial velocity, for a significant wave height of $H_s = 1$ m. The uncontrolled pendulum responses with transitory counter-clockwise rotations due to the high value of $\dot{\theta}_0$, but soon these rotations lose. For the controlled pendulum, as long as the response is naturally rotational

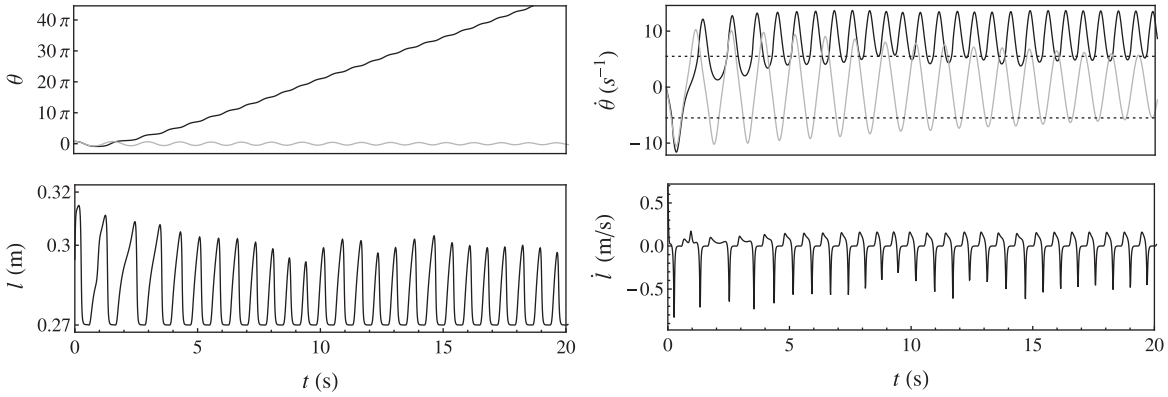

Fig. 7. Comparison between controlled (—) and uncontrolled (▬) responses of the parametric pendulum for stochastic forcing $Y(t)$ given by Eq. (6). $n = 50$, $H_s = 2.0$ m, $\Omega_N = 4$ s^{-1}. Initial conditions: $\theta_0 = 3\pi/4$, $\dot{\theta}_0 = 0.01$ s^{-1}. Steepness factors: $k = 3.5$, $k_L = 0.99$. Threshold factor: $\alpha_L = 0.55$, (. . .): $\dot{\theta}_L = 6.7$ s^{-1}. Counterclockwise rotations are successfully obtained from oscillations due to the control action.

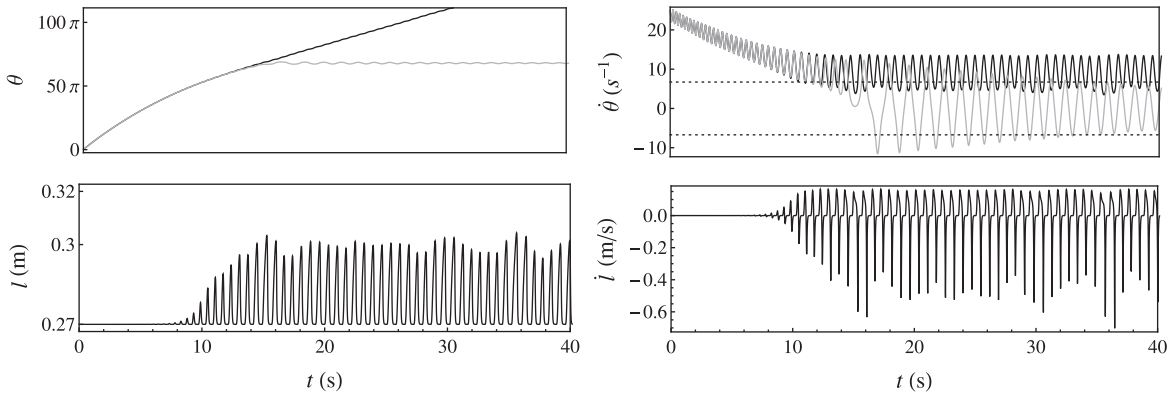

Fig. 8. Comparison between controlled (—) and uncontrolled (▬) responses of the parametric pendulum for stochastic forcing $Y(t)$ given by Eq. (6). $n = 50$, $H_s = 1.0$ m, $\Omega_N = 4\,s^{-1}$. Initial conditions: $\theta_0 = \pi/4$, $\dot{\theta}_0 = 25\,s^{-1}$. Steepness factors: $k = 3.5$, $k_L = 0.99$. Threshold factor: $\alpha_L = 0.55$, (. . .): $\dot{\theta}_L = 6.7\,s^{-1}$. The transitory response corresponds to a counterclockwise rotational motion. When rotations seem to lose, a control action prevents it.

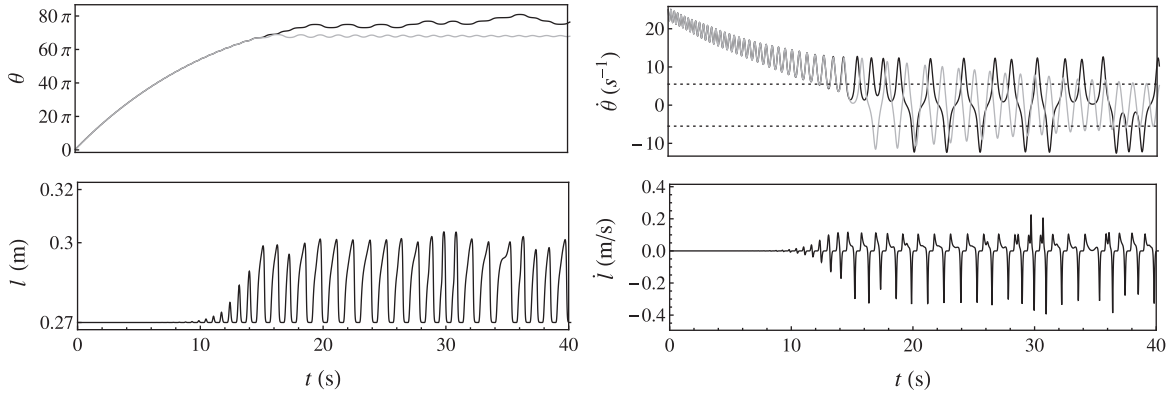

Fig. 9. Comparison between controlled (—) and uncontrolled (▬) responses of the parametric pendulum for stochastic forcing $Y(t)$ given by Eq. (6). $n = 50$, $H_s = 1.0$ m, $\Omega_N = 4\,s^{-1}$. Initial conditions: $\theta_0 = \pi/4$, $\dot{\theta}_0 = 25\,s^{-1}$. Steepness factors: $k = 3.5$, $k_L = 0.99$. Threshold factor: $\alpha_L = 0.35$, (. . .): $\dot{\theta}_L = 5.5\,s^{-1}$. The transitory response corresponds to a counterclockwise rotational motion. When rotations seem to lose, a control action tries to prevent it. But the threshold velocity $\dot{\theta}_L$ is too small and thus the control fails.

(up to $t \cong 14$ s), the control is not operative. When $\dot{\theta}$ drops below $\dot{\theta}_L$, a control action starts to maintain rotations.

The lowest possible $\dot{\theta}_L$ is desirable since it allows saving energy in the control operation (the control operates during less time). But an excessively low $\dot{\theta}_L$ can result in an impossibility to reach stable rotations. A scenario with identical forcing conditions as the previous example is presented in Fig. 9, with the only difference of $\dot{\theta}_L$, which is reduced from 6.7 s^{-1} to 5.5 s^{-1}. It can be observed that, being $\dot{\theta}_L$ too small, the control action is insufficient to maintain the rotational motion. Instead of rotations, tumbling chaos is obtained [17].

As in the previous section, many more simulations were conducted for several initial conditions and values of H_s and N. In all cases, successful results were obtained with $0.5 < \alpha_L < 1$ (i.e. a sufficiently high percentage of $\dot{\theta}_L$). Small modifications of the steepness factors k and k_L are required for some loading scenarios in order to obtain a realistic value of the actuator velocity $\dot{l}$. With a view on a real application, k and k_L must be set based on experimental measures of the waves where the harvester needs to be installed.

5. Conclusions

Among the many possible dynamic responses of the vertically excited parametric pendulum, stable rotations are the most desirable in regard to energy harvesting, because of their high energy [11]. But stable rotations are proved hard to obtain, even with a simple sinusoidal excitation, and this is due to the strong dependency of the dynamical system on forcing parameters and initial conditions [17]. In this article, we introduce a control strategy for the parametric pendulum, with aim to achieve stable rotations under any time-dependant forcing condition. The idea is to give the pendulum an aid to reach and maintain rotations by means of a telescopic adjustment of the length during the motion [20]. This adjustment modifies the position of the mass according to a convenient strategy, resulting in an acceleration of the motion. The control function proposed is based on the logistic and sine functions, and uses as input the angular position and velocity of the pendulum.

Two possible energy sources are considered: a vibrating machine, represented by a sinusoidal excitation; and the sea waves, simulated by a stochastic process. The results of numerical simulations show that, if a threshold velocity is adequately chosen to regulate the control action, the controlled pendulum is able to reach stable rotations for both forcing scenarios, irrespective of the initial conditions and forcing parameters.

This is, however, an idea at the formative stage with experiments still ongoing. There are unanswered questions about the practical implementation of the technology and the minimization of the energy required by the control system, energy which must be extracted from the generation. We know these are issues which can lead to drawbacks, and even to make the implementation unfeasible. But from the good results in the numerical field, we think that it is worth considering the idea. Hopefully, this article can be useful as a vehicle for discussion on the application of this control technique.

Acknowledgements

The authors would like to thank the support of CONICET, Secretary of Science and Technology of Universidad Tecnológica Nacional and Engineering Department of Universidad Nacional del Sur.

References

[1] X.D. Xie, Q. Wang, N. Wu, Energy harvesting from transverse ocean waves by a piezoelectric plate, Int. J. Eng. Sci. 81 (2014) 41–48.
[2] M. Wiercigroch, A new concept of energy extraction from waves via parametric pendulor. UK patent application, 2010.
[3] D. Alghisi, S. Dalola, M. Ferrari, V. Ferrari, Triaxial ball-impact piezoelectric converter for autonomous sensors exploiting energy harvesting from vibrations and human motion, Sens. Actuators A-Phys. 233 (2015) 569–581.
[4] G. Gatti, M.J. Brennan, M.G. Tehrani, D.J. Thompson, Harvesting energy from the vibration of a passing train using a single-degree-of-freedom oscillator, Mech. Syst. Signal Process. 66–67 (2016) 785–792.
[5] V. Ostasevicius, V. Markevicius, V. Jurenas, M. Zilys, M. Cepenas, L. Kizauskiene, V. Gyliene, Cutting tool vibration energy harvesting for wireless sensors applications, Sens. Actuators A-Phys. 233 (2015) 310–318.
[6] S.R. Anton, A. Ertuk, D.J. Inman, Energy harvesting from small unmanned air vehicles, in: Proceedings of the 17th international symposium on application of ferroelectrics, vol. 3, 2008, pp. 23–28.
[7] N.G. Stephen, On energy harvesting from ambient vibration, J. Sound Vib. 293 (2006) 409–425.
[8] S.P. Machado, M. Febbo, F. Rubio-Marcos, L.A. Ramajo, M.S. Castro, Evaluation of the performance of a lead-free piezoelectric material for energy harvesting, Smart Mater. Struct. 24 (2015) 115011.
[9] .M. Renno, M.F. Daqaq, D.J. Inman, On the optimal energy harvesting from a vibration source, J. Sound Vib. 320 (2009) 386–405.
[10] K. Nandakumar, M. Wiercigroch, A. Chatterjee, Optimum energy extraction from rotational motion in a parametrically excited pendulum, Mech. Res. Commun. 43 (2012) 7–14.
[11] A. Najdecka, S. Narayanan, M. Wiercigroch, Rotary motion of the parametric and planar pendulum under stochastic wave excitation, Int. J. Nonlinear Mech. 71 (2015) 30–38.
[12] S. Lenci, G. Rega, Experimental versus theoretical robustness of rotating solutions in a parametrically excited pendulum: a dynamical integrity perspective, Phys. D 240 (2011) 814–824.
[13] X. Xu, M. Wiercigroch, Approximate analytical solutions for oscillatory and rotational motion of a parametric pendulum, Nonlinear Dyn. 47 (2007) 311–320.
[14] A. Najdecka, T. Kapitaniak, M. Wiercigroch, Synchronous rotational motion of parametric pendulums, Int. J. Nonlinear Mech. 70 (2015) 84–94.
[15] F.E. Dotti, F. Reguera, S.P. Machado, A review on the nonlinear dynamics of pendulum systems for energy harvesting from ocean waves, in: Proceedings of the 1st Panamerican Congress on computational mechanics (PANACM), Buenos Aires, Argentina, 2015, pp. 1516–1529.
[16] A. Souza de Paula, M.A. Savi, Controlling chaos in a nonlinear pendulum using an extended time-delayed feedback control method, Chaos Soliton. Fract. 42 (2009) 2981–2988.
[17] M.J. Clifford, S.R. Bishop, Rotating periodic orbits of the parametrically excited pendulum, Phys. Lett. A 201 (1995) 191–196.
[18] W. Garira, S.R. Bishop, Rotating solutions of the parametrically excited pendulum, J. Sound Vib. 263 (2003) 233–239.
[19] X. Xu, M. Wiercigroch, M.P. Cartmell, Rotating orbits of a parametrically-excited pendulum, Chaos Soliton. Fract. 23 (2005) 1537–1548.
[20] M.C. Pereira, H.I. Weber, Analysis of the oscillation of a self-excited pendulum due to varying length, in: Proceedings of the 1st Panamerican Congress on computational mechanics (PANACM), Buenos Aires, Argentina, 2015, pp. 272–280.
[21] R.W. Leven, B.P. Koch, Chaotic behaviour of a parametrically excited damped pendulum, Phys. Lett. A 86 (1981) 71–74.
[22] M. Shinozuka, C.-M. Jan, Digital simulation of random processes and its applications, J. Sound Vib. 25 (1) (1972) 111–128.
[23] W.J. Pierson, Wind generated gravity waves, Adv. Geophys. 2 (1955) 93–178.
[24] S. Lenci, G. Rega, Competing dynamic solutions in a parametrically excited pendulum: attractor robustness and basin integrity, J. Comput. Nonlinear Dyn. 3 (2008) 041010.
[25] J.M.T. Thompson, H.B. Stewart, Nonlinear Dynamics and Chaos, John Wiley & Sons, West Sussex, 2003.
[26] R.W. Leven, M. Selent, D. Uhrlandt, Fractal dimensions and $f(\alpha)$ spectrum of chaotic sets near crises, Chaos Soliton. Fract. 4 (5) (1994) 661–676.